AD-A117 394 ARMY ARMAMENT RESEARCH AND DEVELOPMENT COMMAND DOVER--ETC F/G 20/5
CO2 LASER WAVEGUIDING IN GAAS MBE LAYERS.(U)
JUN 82 H A JENKINSON, J M ZAVADA

UNCLASSIFIED NL

END
DATE FILMED
8 82
DTIC

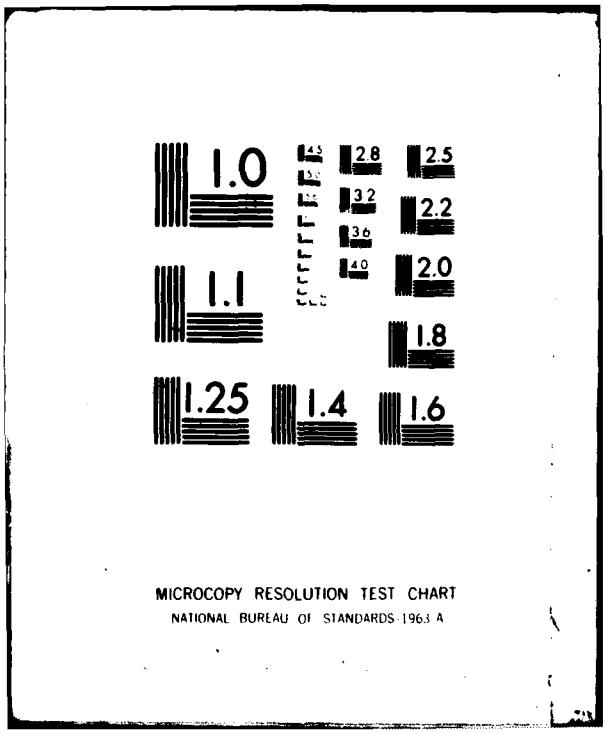
1.0
1.1
1.25
1.4
1.6
1.8
2.0
2.2
2.5
2.8
3.2
3.6
4.0
MICROCOPY RESOLUTION TEST CHART
NATIONAL BUREAU OF STANDARDS-1963-A

18 JUN 1982

CO_2 LASER WAVEGUIDING IN GaAs MBE LAYERS

* HOWARD A. JENKINSON, MR.
JOHN M. ZAVADA, DR.
Fire Control and Small Caliber
Weapon Systems Laboratory
ARRADCOM, Dover, NJ 07801

I. INTRODUCTION

Integrated optical circuits have vast potential for use as sensing and signal processing elements in future Army fire control systems. One of the requirements for these systems is 24 hour/all weather operation. In order to meet this requirement, the Army has been emphasizing systems which operate at longer wavelengths, in particular, at the 10.6 micron CO_2 laser line. Such systems, including CO_2 laser radars, miss-distance sensors, and sensors for smart munitions form a natural area of application for infrared integrated optical circuits. These circuits could be used to perform various functions including phased array transmission, heterodyne detection, parallel processing and optical correlation. In order to perform these operations it is first necessary to develop efficient waveguides for confining the laser light.(1).

The simplest version of an optical waveguide is a planar structure with an uniform dielectric constant (2). For an electromagnetic wave to be guided in this structure, the dielectric constant must be larger than that of the adjacent media. The guided wave will then propagate in a zig-zag fashion within this structure undergoing total internal reflection at each interface.

There are two main problems with this type of optical waveguide. The first arises from surface and interfacial irregularities that scatter light out of the waveguiding region. This scattering can lead to large propagation losses and to poor signal/noise characteristics. The second is lack of phase coherence for modes of different order. This difficulty limits the use of such structures in multimode propagation and reduces the information content that can be transferred. Similar problems have been encountered with optical fibers used in communication systems and have led to the development of Graded Index (GRIN) or Self-Focusing (SELFOC) fibers (3). The refractive index of these fibers is no longer uniform but varies according to a parabolic profile. Due to this index variation, light rays

in the fiber are contained in a sinusoidal envelope. Since the light ray never touches the interface, scattering losses from surface irregularities are drastically reduced. Also, the index profile is adjusted to maintain phase coherence for a wide range of propagating modes.

While such advances have been made in the fabrication of cylindrical optical fibers, controlled index profiling has not as yet been achieved in planar optical waveguides. The reason for this lies in the considerable difficulty of introducing impurity atoms in a precise manner over a two dimensional region of several square centimers.

Molecular beam epitaxy (MBE) is a vacuum deposition processing technique (4) in which several different atoms or molecules can be deposited producing a film with the same crystalline structure as the substrate (epitaxial growth). MBE machines have been available for over a decade but the quality of the deposited films has often been erratic. Recent progress in vacuum technology has allowed the fabrication of high quality films in a reproducible manner.

With modern MBE machines, it is also possible to grow multilayer planar structures in which the optical properties of individual layers can be accurately controlled through electronic doping. Index tailoring of this type can lead to novel electro-optical devices for use in integrated optics and microelectronics. To effectively utilize the advantages of multilayer structures for guided wave applications, it is necessary to be able to determine the optical waveguiding characteristics of such structures.

In this report, experimental analyses of the electronic and optical properties of a prototype single layer MBE* waveguide are presented. A polished (100) wafer of n^+-GaAs heavily doped with silicon was used as the waveguide substrate. The free carrier concentration was approximately $3 \times 10^{18}/cm^3$. An epitaxial layer of n-GaAs lightly doped with tin was then grown on the substrate. The carrier concentration of the epitaxial layer was targeted to be $3\text{-}5 \times 10^{15}/cm^3$.

*(molecular beam epitaxy)

II. DIELECTRIC MODEL

The dependence of the refractive index on the carrier concentration can be illustrated by a simple dielectric model in which the dielectric function of GaAs is composed of Lorentz oscillator terms representing the lattice contribution (5) and a Drude term representing the depression of the dielectric function due to the presence of the free carriers (6). In the spectral region between the band gap and the IR phonon resonance, the dispersion due to the lattice contribution is much less than that due to the plasma. Thus, to good approximation, the dielectric function may be

written, in terms of wavenumber σ, as

$$n^2(\sigma) = K_L - \frac{\sigma_p^2}{\sigma(\sigma + ig)} \qquad 269\ cm^{-1} \ll \sigma \ll 2x10^4\ cm^{-1} \quad (1)$$

where K_L is the high frequency dielectric constant of GaAs, taken to be 10.73. σ_p is related to the carrier concentration N through

$$\sigma_p^2 = \frac{Ne^2}{(2\pi e)^2 m^* \varepsilon_o} \quad (2)$$

where c is the speed of light, e is the electronic charge, $m^* = .08m_e$ is the effective mass of electrons in GaAs, and ε_o is the vacuum permittivity. The damping factor, g, leads to losses and is related to the mobility, μ, of the material through

$$g = \frac{e}{2\pi c \mu m^*} \quad (3)$$

Neglecting losses, the increase in the refractive index at the substrate-epilayer interface due to the carrier concentration difference is approximately

$$\Delta n \simeq \frac{\sigma_{p,s}^2 (1 - N_f/N_s)}{2n\sigma^2} \quad (4)$$

where $\sigma_{p,s}^2$ is σ_p^2 evaluated using the original carrier concentration N_s of the substrate and N_f is the carrier concentration in the MBE layer.

III. INFRARED REFLECTANCE

Prior to waveguiding experiments the optical properties of the MBE sample were characterized by infrared reflectance measurements. Differential reflectance measurements, made over the spectral range of 4000 cm^{-1} to 1400 cm^{-1}, yielded interference fringes typical of a thin film/substrate structure, as illustrated in Figure 1. The interesting features of this curve are the periodicity of the fringes and their increase in amplitude as the measurement progresses to smaller wavenumbers. A first-order model has been developed to aid in deducing the carrier concentration and the thickness of the epitaxial layer from the reflectance spectrum. Basically, losses are neglected and the layer is considered to be a film of refractive

index n_f sitting atop a substrate whose index has been depressed a small amount Δn by its higher concentration of free carriers. The reference sample is considered identical to the substrate. Expanding the relevant reflectance equations in a McLaurin series expansion to first order in Δn and using equation (4) yields:

$$R_D^2(\sigma) = \frac{R^2_{sample}}{R^2_{reference}} \simeq 1 + \frac{4\sigma_{p,s}^2(1-N_f/N_s)}{n_f(n_f^2-1)}\left(\frac{\sin(2\pi t n_f \sigma)}{\sigma}\right)^2 \qquad (5)$$

From this analysis, it can be shown that the thickness of the epitaxial layer can be determined by the location, σ_m, and order, m, of the fringe minima, and the relative carrier difference, X, by the fringe amplitudes:

$$t = m/(2n_f\sigma_m) \; ; \qquad X = 1 - N_f/N_s = \frac{n_f(n_f^2-1)\sigma^2}{4\sigma_{p,s}^2}(R^2_{D,max}-1) \qquad (6)$$

Table 1 presents the reflectance data for the fringe minima located between 1400 and 3000 cm^{-1} that appear in Figure 1. The order of each fringe is identified by dividing its location by the average separation of the fringes in the interval. Using a value of $3.28 = \sqrt{K_L}$ for n_f the thickness of the epitaxial layer was calculated to be 11.45 microns with a standard deviation of .03 microns. The low valve of the standard deviation is due to the uniform periodicity of the reflectance fringes which in turn implies that the epitaxial layer is optically homogeneous. The growth in fringe amplitudes shown in Figure 1 is consistent with the electronic model for the refractive index change. It can be seen from equation (5) that the fringe amplitudes are proportional to (1-Nf/Ns). As this factor reaches 90% of its maximum valve for Nf = .1 Ns, the method is not suitable for accurate determination of epilayer carrier concentrations which are more than an order of magnitude lower than in the substrate.

IV. CV PROFILING

Since reflectance measurements can not determine relatively low carrier concentrations, it is necessary to resort to electronic techniques to measure Nf. One suitable method is that of capacitance voltage (C-V) profiling. This technique is based on the principle that a Schottky barrier (metal-semiconductor interface) formed on the surface of the epitaxial layer will behave like a parallel plate capacitor. In this picture one plate of the capacitor is formed by the Schottky barrier, the other is formed by the free carriers within the epitaxial layer. As the Schottky barrier is reversed biased, the free carriers in the epilayer are repelled, causing the moveable "plate" to recess further into the epilayer and resulting in a decrease in the measured capacitance. From measurements

of the rate at which the capacitance C decreases as a function of bias voltage V, the carrier concentration as a function of depth can be determined. The equations that describe this measurement technique are (7):

$$W = \varepsilon\varepsilon_o A/C(V) \quad ; \quad N(V) = \left(-\frac{e\varepsilon\varepsilon_o A^2}{2} \frac{d}{dV} \frac{1}{C^2(V)} \right)^{-1} \qquad (7)$$

Here ε is the low frequency dielectric constant, taken to be 12.5 for GaAs, A is the area of the Schottky barrier electrode, and W is the depletion width of the junction. If N is sufficiently low, then it is possible to bias the junction such that the transition region between the epilayer and the substrate can be profiled. The results of such a measurement, made at 1MHz with a gold Schottky barrier vacuum deposited through a stainless steel mask, are shown in Figure 2. This curve indicates that the carrier concentration is uniform throughout the epitaxial layer at a level of approximately $1.6\text{x}10^{15}/\text{cm}^3$. The sharp rise in this curve at a depth of 10.89 micrometers represents the transition to the more heavily doped substrate.

V. INFRARED OPTICAL WAVEGUIDING

Since the reflectance spectra and the CV profile support the approximation of a single dielectric film/substrate structure, the equations for a planar asymmetric dielectric waveguide were used as the waveguide model: (1,2)

$$kt\sqrt{n_f^2-(\beta/k)^2} - \Phi_{fo} - \Phi_{fs} = m\pi \qquad (8)$$

where $k=2\pi/\lambda_o$, $\beta/k=n_f \sin\theta_f$ and the phase angles are defined by:

$$\tan\Phi_{fi}^{TE} = \left(\frac{(\beta/k)^2-n_i^2}{n_f^2-(\beta/k)^2} \right)^{1/2} \quad ; \quad \tan\Phi_{fi}^{TM} = (n_f/n_i)^2 \tan\Phi_{fi}^{TE} \qquad (9)$$

The subscript i refers to either the cover layer o or to the substrate s. Equation (8) is the familiar eigenvalue condition which must be satisfied for optical waveguiding to occur and is expressed in terms of the ratio β/k. This factor can be interpreted as the effective refractive index of the waveguide for each mode and is restricted to values between n_s and n_f. Based on the dielectric model, these parameters are expected to be 2.64 and 3.28 respectively at 10.6 microns.

Infrared optical waveguiding was achieved in this sample using a 1 watt

CO_2 laser operating at 10.6 microns. The radiation was focused through an f-10 ZnSe lens on a dove shaped germanium prism which effected coupling into and out of the waveguide. The emerging beam, totally internally reflected from the base of the prism, was imaged as a spot on a thermographic screen. Waveguiding was identified by an absorption notch in the reflected spot, indicating that radiation was removed from the incident beam. Measurements of the angles at which synchronous coupling was achieved were made for both s and p polarizations of the incident beam.

Experimentally, the TE modes were much easier to observe than the TM modes. This is due to the greater amount of energy that can be coupled into the modes. A total of eight modes, five TE and three TM, were observed and Table 2 contains the experimental results. In principal, the coupling data from any two of these modes can be used to numerically invert the mode equations to obtain the refractive index and thickness of the epitaxial layer. Since there was a larger degree of uncertainty in the TM measurements listed in Table 2, only the TE coupling data were used for this purpose. From these measurements, the refractive index of the epitaxial layer was calculated to be 3.27 with a standard deviation of .01 and the thickness to be 12.19 microns with a standard deviation of .23 microns.

VI. DISCUSSION

The results of these three independent measurements are summarized in Table 3. In the IR reflectance and CV profiling measurements, it is necessary to postulate a dielectric model for n-type GaAs in order to relate the experimental data to the optical properties of the epitaxial layer. The synchronous coupling experiments, however, provide a direct determination of n_f through the waveguiding equations. The excellent agreement of the three determinations of n_f supports the validity of the dielectric model, and indicates that the free carrier concentration is the dominant mechanism responsible for the refractive index change.

The thickness determinations are also in good agreement, but are more subject to systematic measurement errors arising in the different experimental techniques. The IR reflectance determination was calculated from a first order approximation to the exact mathematical expression for the reflectance of a thin film-substrate structure. Hence, the absolute error may be larger than indicated by the standard deviation. The C-V determination involves precise measurements of small values of capacitance and the electrode area. Experimental uncertainties in these quantities limit the overall accuracy of the thickness determination to 5%. Furthermore, the optical thickness is determined by the depth at which the carrier concentration rises from 10% to 100% of the substrate concentration. This region was not completely probed in the current experiments. The

synchronous coupling determination is again a direct measurement and may be more representative of the actual thickness of the layer in spite of the larger standard deviation. Finally, it is possible that the transition region from the MBE layer to the substrate will ultimately be shown to have a carrier concentration gradient extending over a few thousand Angstroms. This would lead to a graded index layer which would necessitate data interpretation with more complex models than used here.

While molecular beam epitaxy is still an emerging technology, the present experiments show that it can be used to form high quality CO_2 laser waveguiding structures. The epitaxial layer examined in this study displayed very uniform optical and electronic properties that can be related to an elementary Lorentz-Drude dielectric model. These results substantiate using this model to design more complicated graded index CO_2 waveguides through MBE.

ACKNOWLEDGEMENT

The authors wish to thank J. Comas of the Naval Research Laboratory for providing the MBE sample used in this investigation.

VII. REFERENCES

1. J. M. Zavada, H. A. Jenkinson, T. J. Gavanis, R. G. Hunsperger, D. C. Larson and J. Comas, "Ion Implanted Guided Wave Devices for Army Fire Control," 1980 Army Science Conference Proceedings, Vol. III, 445 (1980).

2. D. Marcuse, Theory of Dielectric Optical Waveguides, Academic Press, New York, 1974.

3. M. S. Sodha and A. K. Ghatak, Inhomogeneous Optical Waveguides, Plenum, New York, 1979.

4. C. E. C. Wood, "Progress, Problems, and Applications of Molecular-Beam Epitaxy," in Physics of Thin Films, Vol. II, Academic Press, 1980.

5. A. H. Kachare, W. G. Spitzer, J. E. Frederickson, and F. K. Euler, "Measurements of Layer Thicknesses and Refractive Indices in High-Energy Ion-Implanted GaAs and Gap." J. Appl. Phys., 47, no. 12, 5374 (1976).

6. J. M. Zavada, H. A. Jenkinson, and T. J. Gavanis, "Optical Properties of Proton Implanted n-Type GaAs," Proc. Soc. Photo-Optical Instrum. Eng., 276, 104 (1981).

7. A. Glasser and G. Subak-Sharpe, Integrated Circuits Engineering, Addison-Wesley, Reading, 1977.

Table 1. IR REFLECTANCE DATA: GaAs MBE 8126

σ_m (cm^{-1})	m	σ_m/m (cm^{-1})	(micrometers)
2925	22	132.95	11.466
2790	21	132.86	11.474
2655	20	132.75	11.483
2530	19	133.16	11.448
2390	18	132.78	11.481
2260	17	132.94	11.467
2135	16	133.44	11.424
1995	15	133.00	11.462
1865	14	133.21	11.444
1735	13	133.46	11.422
1605	12	133.75	11.397
1470	11	133.64	11.407

Table 2. SYNCHRONOUS COUPLING DATA AT 10.6 MICRONS: GaAs MBE 8126

MODE	β/k
TE_o	3.249
TM_o	-
TE_1	3.175
TM_1	3.173
TE_2	3.051
TM_2	3.038
TE_3	2.878
TM_3	2.847
TE_4	2.667
TM_4	-

Table 3. SUMMARY OF MEASUREMENT RESULTS: GaAs MBE 8126

	CARRIER CONCENTRATION ($1/cm^3$)	REFRACTIVE INDEX 10.6 um	THICKNESS (um)
Substrate (Manuf. Spec)	3.0×10^{18}	2.64	-
Film-IR Reflectance	$<1 \times 10^{17}$	3.28	$11.45 \pm .03$
C-V Profile	1.6×10^{15}	3.28	10.89
Synchronous Coupling	$<1 \times 10^{17}$	$3.27 \pm .01$	$12.19 \pm .23$

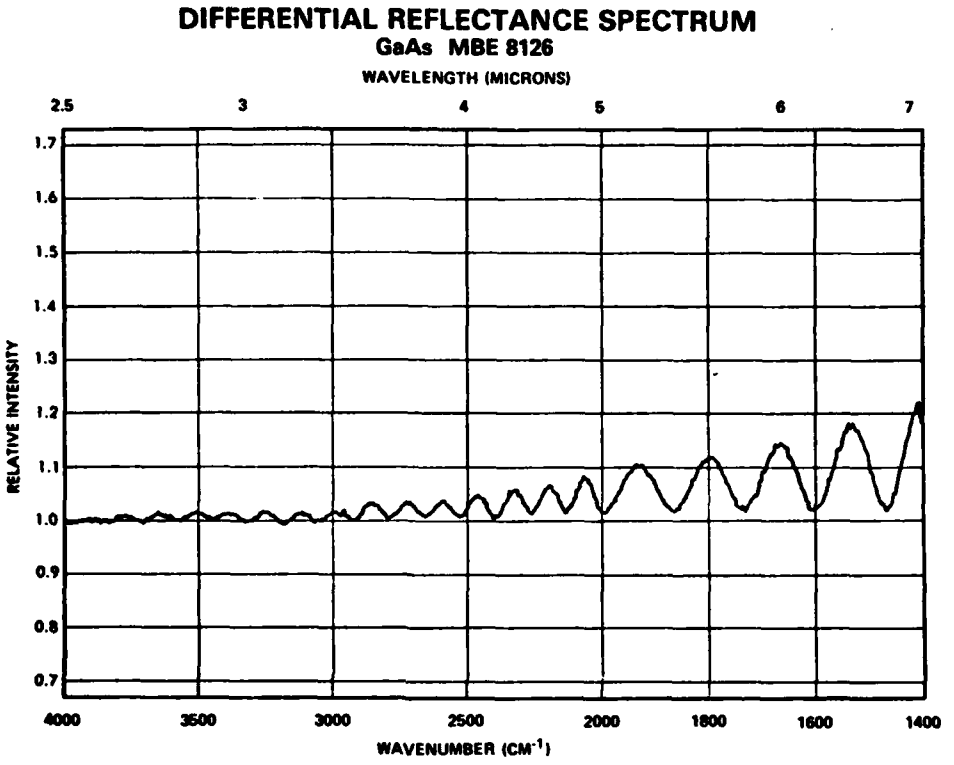
DIFFERENTIAL REFLECTANCE SPECTRUM
GaAs MBE 8126
WAVELENGTH (MICRONS)
2.5
3
4
5
6
7
1.7
1.6
1.5
1.4
1.3
1.2
1.1
1.0
0.9
0.8
0.7
RELATIVE INTENSITY
4000
3500
3000
2500
2000
1800
1600
1400
WAVENUMBER (CM-1)

Figure 1.

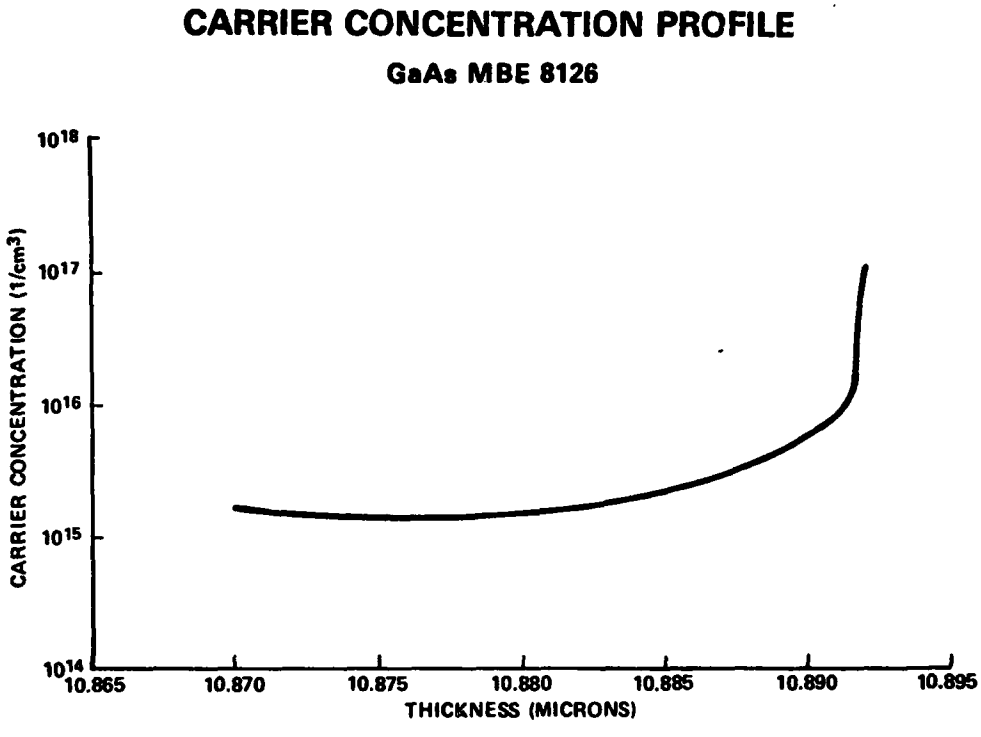
CARRIER CONCENTRATION PROFILE
GaAs MBE 8126
CARRIER CONCENTRATION (1/cm³)
10¹⁸
10¹⁷
10¹⁶
10¹⁵
10¹⁴
10.865
10.870
10.875
10.880
10.885
10.890
10.895
THICKNESS (MICRONS)

Figure 2.